Symbol time offset estimation in coherent OFDM systems

Landström, Daniel; Wilson, S.K.; van de Beek, J.J.; Ödling, Per; Börjesson, Per Ola

Published in:
[Host publication title missing]

DOI:
10.1109/ICC.1999.767990

1999

Symbol time offset estimation in coherent OFDM systems

Daniel Landström[1] Sarah Kate Wilson[2] Jan-Jaap van de Beek[3] Per Ödling[1]
Per Ola Börjesson[1]

[1] Lund University, Dept. of Applied Electronics, SE-221 00 Lund, Sweden
[2] Luleå University, Div. of Signal Processing, SE-971 87 Luleå, Sweden
[3] Nokia Svenska AB, Box 1070, SE-164 25 Kista, Sweden

Abstract

This paper presents a symbol time offset estimator for coherent OFDM systems. This estimator exploits both the redundancy in the cyclic prefix and the pilot symbols used for channel estimation. The estimator is robust against frequency offsets and is suitable for use in dispersive channels. We base the estimator on the ML estimator for the AWGN channel. Simulations of an example system indicate a system performance as close as 0.3 dB to a perfectly synchronized system. Compared to an estimator not using pilots, our estimator's performance could allow a shorter cyclic prefix and thus a more spectrally efficient system.

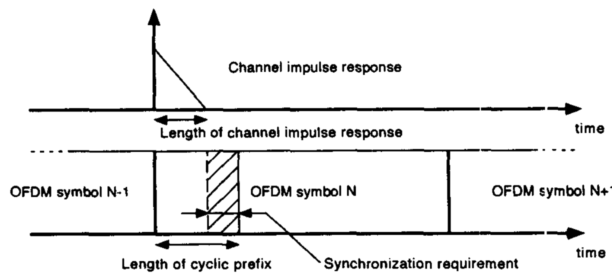

Figure 1: The time offset requirements. As long as the time offset is in the striped area ISI and ICI can be avoided.

1 Introduction

Most coherent *orthogonal frequency-division multiplexing* (OFDM) systems, such as the *Digital Video Broadcast* (DVB) system [1] and future multiuser systems currently under investigation [2, 3], use pilot symbols to estimate the channel [4, 5]. In this paper we present a method of using these pilot symbols for symbol time synchronization. We present a new time offset estimator that exploits both the redundancy introduced by the cyclic prefix and the channel estimation pilots. Its performance allows for a tight design of the cyclic prefix improving the spectral efficiency of the system.

First, we derive the *maximum likelihood* (ML) estimator for a symbol time offset in coherent OFDM systems. It is based on a suitably chosen model of the OFDM symbol, emphasizing the cyclic prefix redundancy and the presence of pilots, but disregarding channel dispersion, frequency offset, and signal correlation. This estimator is, however, very sensitive to variations in the carrier frequency. Based on the ML estimator and on earlier results in [6], we present a new *ad hoc* estimator that is robust against frequency offsets and suitable for practical systems. This new robust estimator shows good performance in a dispersive environment.

Synchronization is a critical problem in OFDM systems, and the effects of synchronization errors are documented in, *e.g.*, [7, 8]. The requirements for the time offset estimator are determined by the difference in length between the cyclic prefix and the channel impulse response. This difference is the part of the cyclic prefix that is not affected by the previous symbol due to the channel dispersion, as shown in Figure 1. As long as a symbol time offset estimate does not exceed this difference, the orthogonality of the subcarriers is preserved, and a time offset within this interval only results in a phase rotation of the subcarrier constellations. In the case of pilot based coherent modulation, this phase shift will be compensated for by a frequency-domain channel equalizer. The closer the time-offset estimate is to the true offset, the shorter the cyclic prefix needs to be, reducing the overhead in the system.

This paper proceeds as follows. In Section 2 we describe our signal model and our model assumptions. In Section 3 we derive the ML time offset estimator and present the robust estimator. We evaluate their performance in Section 4 and present our conclusions in Section 5.

0-7803-5284-X/99/$10.00 © 1999 IEEE.

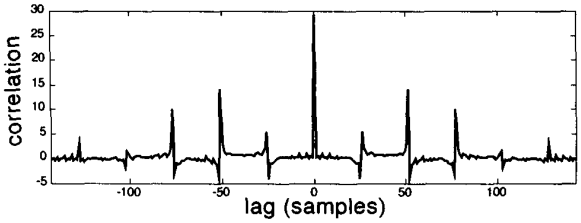

Figure 2: The real part of a typical pilot symbol's autocorrelation function, $N = 128$, $L = 16$, and 1 pilot every 5th subcarrier.

2 The signal model

In OFDM systems the data is modulated in blocks by means of a *discrete Fourier transform* (DFT). By inserting a cyclic prefix in the OFDM symbol, *intersymbol interference* (ISI) and *intercarrier interference* (ICI) can be avoided, and the orthogonality between subcarriers is maintained [9]. Most coherent OFDM systems transmit pilot symbols on some of the subcarriers to measure the channel attenuations [4]. Both the cyclic prefix and the channel estimation pilots contain information about the symbol start, which can be exploited. We show here that it may not be necessary to insert additional pilots for synchronization.

Assume that one transmitted OFDM symbol consists of N subcarriers of which N_p are modulated by pilot symbols. Let $\mathcal{N}$ denote the set of indexes of the N_p pilot carriers. We separate the transmitted signal in two parts. The first part contains the $N - N_p$ data subcarriers and is modelled by

$$s(k) = \frac{1}{\sqrt{N}} \sum_{n \in \{0,..,N-1\} \setminus \mathcal{N}} x_n e^{-j2\pi kn/N}, \quad (1)$$

where x_n is the data symbol transmitted on the nth subcarrier, using some constellation with average energy $\sigma_x^2 = E\{|x_n|^2\}$. The second part contains the N_p pilot subcarriers, modelled by

$$m(k) = \frac{1}{\sqrt{N}} \sum_{n \in \mathcal{N}} p_n e^{-j2\pi kn/N}, \quad (2)$$

where p_n is the pilot symbol transmitted on the nth subcarrier. We assume $E\{|p_n|^2\} = \sigma_x^2$, although some systems have boosted pilots [1]. Figure 2 shows the real part of the autocorrelation function for a typical pilot signal $m(k)$ for a system with $N = 128$ subcarriers where every fifth subcarrier contains a pilot symbol. Notice that the IDFT of the pilots symbols, $m(k)$, has a distinct correlation which we can exploit.

In the following we assume an *additive white Gaussian noise* (AWGN) channel and we model the received signal $r(k)$ as

$$r(k) = s(k - \theta) + m(k - \theta) + n(k), \quad (3)$$

where θ represents the unknown integer-valued time offset and $n(k)$ is additive complex white zero-mean Gaussian receiver noise with variance σ_n^2. Two properties of the received signal allow for the estimation of θ: the statistical properties of $s(k)$ and the knowledge of $m(k)$.

In two steps we choose to simplify the statistical properties of $s(k)$ compared to those of signal (1), so that we can derive a tractable estimator. First, in an OFDM system with a reasonably large number of data-carrying subcarriers ($N_p \ll N$), $s(k)$ has statistical properties similar to a discrete-time Gaussian process (by the Lindeberg theorem [10, pp. 368–369]). In our model we assume that the transmitted signal $s(k)$ is a Gaussian process with variance $\alpha\sigma_x^2$, where $\alpha = \frac{N-N_p}{N}$. Secondly, we simplify the statistical properties of $s(k)$ with respect to its correlation. In systems employing a cyclic prefix, the tail L samples of the N-sample ($L < N$) transmitted signal $s(k) + m(k)$ are copied, *i.e.*, $s(k) = s(k + N)$, and $m(k) = m(k + N)$, for $k \in [0, L-1]$. The length of one OFDM symbol is thus $N+L$ samples of which L samples constitute the cyclic prefix. Therefore, $s(k)$ is not white but contains pairwise correlations between samples spaced N samples apart. Furthermore, $s(k)$ is correlated because not all tones are used for data. For most practical systems, however, this latter correlation will be small if the number of pilots is small. Whereas we do model the correlation due to the cyclic prefix, we disregard any correlation of the latter kind.

Since the noise is zero-mean Gaussian and the pilot signal $m(k)$ is a deterministic signal which is known at the receiver, the modelled received signal $r(k)$ is also Gaussian with time-varying mean $m(k)$ and variance $\alpha\sigma_x^2$. Because of the cyclic prefix, its autocorrelation function is

$$c_r(k,l) = \begin{cases} 1 & k - l = 0 \\ \rho & k - l = -N, k \in [\theta, \theta + L - 1] \\ \rho & k - l = N, l \in [\theta, \theta + L - 1] \\ 0 & \text{otherwise} \end{cases}, \quad (4)$$

where

$$\rho = \frac{\alpha\sigma_x^2}{\alpha\sigma_x^2 + \sigma_n^2} = \frac{\alpha\text{SNR}}{\alpha\text{SNR} + 1}, \quad (5)$$

and $\text{SNR} = \frac{\sigma_x^2}{\sigma_n^2}$ is the *signal-to-noise ratio.*

Based on this correlation structure and on the knowledge of the time-varying mean $m(k)$ we now derive an estimator of the time offset θ, using data from one received OFDM symbol.

3 Time offset estimation

Based in the model (3), we derive the ML estimator of the time offset θ by investigating the log-likelihood function of θ, *i.e.*, the joint probability of the received samples $r(\cdot)$ given θ,

$$\Lambda(\theta) = \Pr\{r(\cdot)|\theta\}. \quad (6)$$

We follow the same procedure as in [6]. The ML time offset estimate θ is obtained by maximizing the log-likelihood function over all possible values of θ,

$$\widehat{\theta}_{\mathrm{ML}} = \arg\max_{\theta}\{\Lambda(\theta)\}. \tag{7}$$

In Appendix A $\Lambda(\theta)$ is shown to be

$$\Lambda(\theta) = \rho\Lambda_{cp}(\theta) + (1-\rho)\Lambda_p(\theta), \tag{8}$$

$$\begin{aligned}\Lambda_{cp}(\theta) &= \mathrm{Re}\left\{\sum_{k=\theta}^{\theta+L-1} r^*(k)r(k+N)\right\} \\ &\quad -\frac{\rho}{2}\sum_{k=\theta}^{\theta+L-1} |r(k)|^2 + |r(k+N)|^2,\end{aligned}$$

reflects the redundancy in the received signal due to the cyclic prefix and

$$\begin{aligned}\Lambda_p(\theta) &= (1+\rho)\mathrm{Re}\left\{\sum_k r^*(k)m(k-\theta)\right\} \\ &\quad -\rho\mathrm{Re}\left\{\sum_{k=\theta}^{\theta+L-1}(r(k)+r(k+N))^*\,m(k-\theta)\right\},\end{aligned}$$

reflects the information carried by the pilot symbols. The function $\Lambda_{cp}(\theta)$ essentially correlates samples spaced N samples apart thus identifying the position of the cyclic prefix, while the function $\Lambda_p(\theta)$ contains a filter matched to the pilots. The estimator (7) then weighs the information carried by the signal's redundancy and the pilot information depending on the value of ρ, which in turn is given by the SNR.

Figure 3 illustrates this for an example OFDM system with 128 subcarriers and a cyclic prefix of 16 samples. Every 8th subcarrier contains a pilot symbol. For an SNR of 8 dB, Figure 3 shows the contributions $\Lambda_{cp}(\theta)$, $\Lambda_p(\theta)$ and the log-likelihood function $\Lambda(\theta)$. Note how the contributions $\Lambda_{cp}(\theta)$ and $\Lambda_p(\theta)$ support each other. The contribution from the cyclic prefix gives an unambiguous but coarse estimate. The contribution from the pilots has very distinct peaks, but would by itself yield an unacceptable ambiguity. The evenly spaced pilots result in many correlation peaks. Together, however, they properly weighted contributions yield an unambiguous and distinct peak in the log-likelihood function. The peaks of $\Lambda_p(\theta)$ fine-tune the coarse estimate based on $\Lambda_{cp}(\theta)$.

For a large SNR ($\rho \approx 1$), the estimate is mainly based on the cyclic prefix redundancy, whereas for a low SNR ($\rho \approx 0$) the estimate relies more on the pilot symbols. If the transmitted signal does not contain any pilot symbols, then $N_p = 0$, $m(\cdot) = 0$, and $\rho = \frac{\mathrm{SNR}}{\mathrm{SNR}+1}$. In this case, the ML estimator (8) reduces to the estimator in [6], which only exploits the cyclic prefix redundancy.

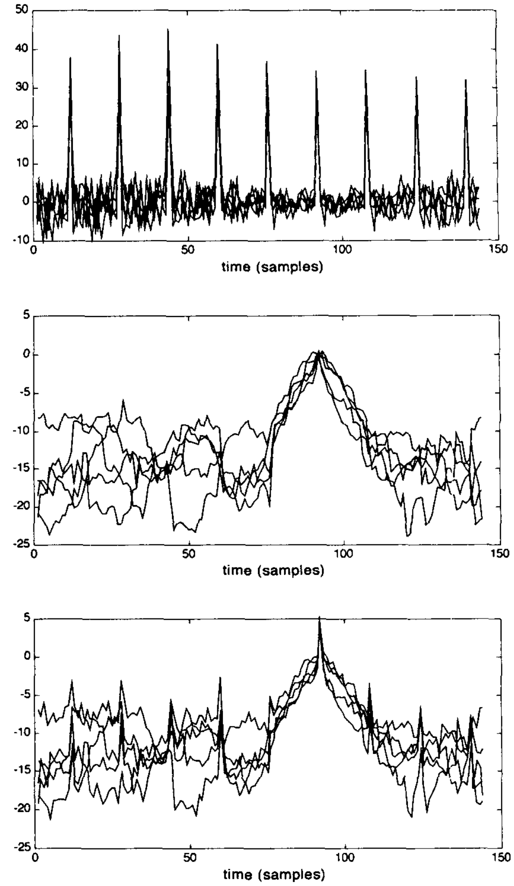

Figure 3: The ML estimator statistics in an AWGN channel. Contribution from the pilots $\Lambda_p(\theta)$ (top), contribution from the cyclic prefix $\Lambda_{cp}(\theta)$ (middle) and the resulting log-likelihood function $\Lambda(\theta)$ (bottom). One OFDM symbol ($N+L$) is 144 samples and the SNR is 8 dB.

3.1 A robust estimator

Most communication systems operate in a dispersive channel and radio-based communication systems often operate with a frequency offset. Figure 4 shows how a normalized frequency offset ϵ (normalized to the subcarrier spacing) affects the performance of the estimator. The simulation is based on $N = 128$ subcarriers, a cyclic prefix of $L = 16$ samples, with 1 pilot every 32nd subcarrier (4 pilot subcarriers in total), and the SNR = 10. We choose $\widetilde{\mathrm{SNR}} = 5$ dB as the design SNR for the robust estimator. Even for small frequency offsets, the performance of the ML estimator decreases significantly. The ML estimator is so sensitive to this distortion that it is of little value in many practical systems. For example, the estimator from [6] (reference estimator) performs better under frequency offsets larger than 0.2 %, as shown in Figure 4. This estimator, which is based only on the cyclic prefix part Λ_{cp} of (8), will be

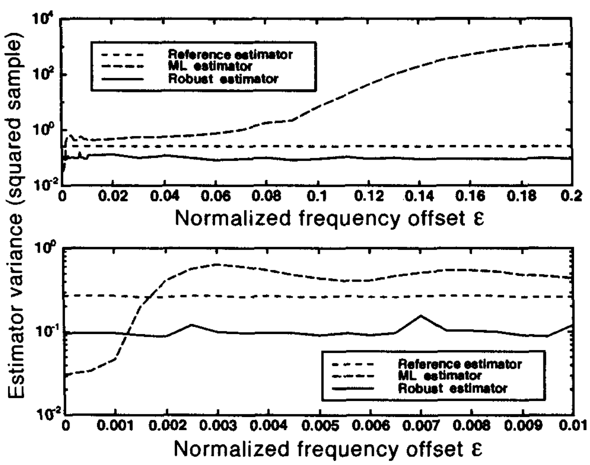

Figure 4: Sensitivity to frequency offsets in an AWGN channel. SNR = 10 dB, $N = 128, L = 16$, 1 pilot every 32nd subcarrier (total: 4 pilot subcarriers), and $\widetilde{\text{SNR}} =$ 5 dB. The reference estimator [6] (coarsely dashed), the ML estimator (7) (fine dashed), and the robust estimator (9) (solid).

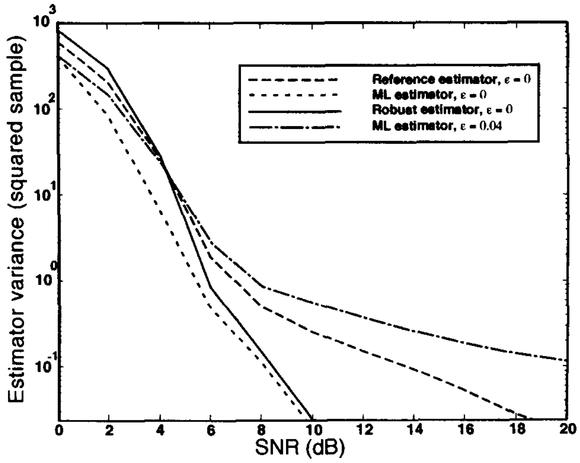

Figure 5: The performance in an AWGN channel, $N = 128, L = 16$, 1 pilot every 32nd subcarrier (total: 4 pilot subcarriers), and $\widetilde{\text{SNR}} = 5$ dB. Note that the ML estimator (7) with a 4% frequency offset (dash-dotted) has been included. If the curves for the robust and the reference estimators were plotted for 4% frequency offset, the curves would be indistinguishable from the curves with no frequency offset.

used as a reference estimator throughout the paper.

Therefore, we propose a robust estimator based on the ML estimator (7) which we modify in two steps. First, because of frequency offsets or channel phase variations, the phases of the peaks in the complex-valued moving sums in (8) appear in a random manner. Based on [6], we take the absolute value of the terms in the log-likelihood function instead of the real part, thus preserving the constructive contribution of the peaks to $\Lambda(\theta)$. In this way we compensate for an unknown frequency offset. Secondly, since the SNR may not be known at the receiver, we design a generic estimator assuming a fixed SNR, which we denote with $\widetilde{\text{SNR}}$.

We choose this design-value lower than the typical SNR we expect, to maintain adequate performance for low-end SNRs in a fading channel. Effectively, this weighs the contribution from the pilots higher than the ML estimator would. We choose the robust estimator as

$$\widehat{\theta}_{\text{ML}} = \arg\max_{\theta}\{\tilde{\rho}\tilde{\Lambda}_{cp}(\theta) + (1-\tilde{\rho})\tilde{\Lambda}_p(\theta)\}, \tag{9}$$

where $\tilde{\rho}$ is a fixed design parameter $\tilde{\rho} = \frac{\alpha\widetilde{\text{SNR}}}{\alpha\widetilde{\text{SNR}}+1}$, and

$$\begin{aligned}\tilde{\Lambda}_{cp}(\theta) &= \left|\sum_{k=\theta}^{\theta+L-1} r^*(k)r(k+N)\right| \\ &\qquad -\frac{\tilde{\rho}}{2}\sum_{k=\theta}^{\theta+L-1} |r(k)|^2 + |r(k+N)|^2, \\ \tilde{\Lambda}_p(\theta) &= (1+\tilde{\rho})\left|\sum_k r^*(k)m(k-\theta)\right| \\ &\qquad -\tilde{\rho}\left|\sum_{k=\theta}^{\theta+L-1} (r(k)+r(k+N))^* m(k-\theta)\right|.\end{aligned}$$

The estimator differs from the estimator in (??) only in the absolute values and the generic choice of $\tilde{\rho}$. The estimator (9) is robust against frequency offsets, as shown in Figure 4.

4 Simulations

We evaluate the estimators' performance by simulations, both in the AWGN channel and in a dispersive channel, showing the variance of the estimates and by symbol error rate. In all simulations, we use the estimator from [6] as our reference estimator.

For the same parameters as in Figure 4, Figure 5 shows the performance of the estimators in an AWGN channel. The ML estimator and the proposed estimator, that use the pilots, have superior performance compared to the reference estimator. As expected, in this environment the ML estimator performs best, but the robust estimator has only a small performance loss for SNR values larger than the design SNR ($\widetilde{\text{SNR}} = 5$ dB). When applying the estimator in an environment with a frequency offset the performance of the ML estimator decreases significantly, as previously seen in Section 3, while the proposed estimator remains applicable.

The symbol error rate of a system employing the estimators in a dispersive channel is shown in Figure 6. The system has $N = 128$ subcarriers, a cyclic prefix of $L = 8$

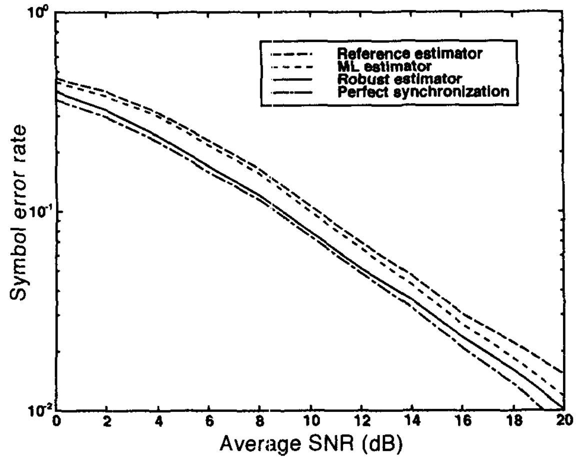

Figure 6: 4-PSK system performance in a dispersive channel, $N = 128, L = 8$, 1 pilot every 5th subcarrier, and $\widetilde{\text{SNR}} = 5$ dB. The channel consists of 8 taps (independently fading according to Jakes' model) with exponentially decaying power-delay profile and rms-value of 2 taps.

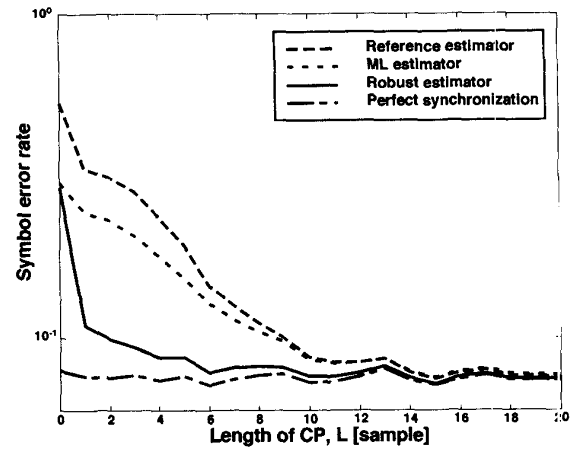

Figure 7: 4-PSK system performance in a dispersive channel, $N = 128$, SNR = 10 dB, 1 pilot every 5th subcarrier, and $\widetilde{\text{SNR}} = 5$ dB. The channel consists of 8 taps (independently fading according to Jakes' model) with exponentially decaying power-delay profile and rms-value of 2 taps.

samples, with 1 pilot every 5th subcarrier, and uses a 4-PSK signal constellation. The channel is exponentially decaying with an rms-value of 2 samples and a length of 8 samples, and is fading according to Jakes' model [11]. As the design SNR for the robust estimator, we choose $\widetilde{\text{SNR}} = 5$ dB. We assume perfect channel knowledge and perfect compensation for the phase rotations of the signal constellation due to time offsets. Thus, we isolate the effect of synchronization errors from possible performance loss due to non-ideal channel estimation. The performance loss shown in Figure 6 is due to ISI and ICI caused by synchronization errors.

We see that the robust estimator now is superior to the others. In this simulation the cyclic prefix and the channel impulse response have the same length, *i.e.*, any synchronization error yields ISI and ICI. Under these tight synchronization requirements the robust estimator has a 0.3 dB loss compared with a perfectly synchronized system at a 10 dB working SNR. For the ML estimator and the reference estimator this loss is 1.3 dB and 1.7 dB, respectively.

Figure 7 shows the estimators' performance as a function of the length of the cyclic prefix. The parameters are the same as in Figure 6 and the SNR = 10 dB. Although the length of the channel is 8 samples, the performance of the reference estimator and the ML estimator starts to decrease for a cyclic prefix shorter than 10 samples, whereas the robust estimator's performance remains low to $L = 5$ samples. From this figure we conclude that, for the purpose of synchronization, it is possible to reduce the cyclic prefix and still preserve the system performance.

5 Discussion and conclusions

As seen in Figure 3, the $\Lambda_p(\theta)$ is an ambiguous function with periodic peaks when the pilots are evenly spaced. By not having the pilots evenly spaced the peaks surrounding the symbol start can be lowered. Therefore the pilot pattern is an interesting design parameter and system design could benefit from taking synchronization aspects into account when designing the channel estimation pilot pattern. To improve performance further, the estimator may be extended by averaging the log-likelihood function or filtering the estimates if the time offset varies slowly in time, see, *e.g.*, [12].

We draw two conclusions from our investigation. First, it is possible to extend the analytic techniques earlier employed in [6] to derive an ML time offset estimator for coherent OFDM systems. Secondly, when also taking the channel estimation pilots into account it is possible to increase the synchronization performance, to decrease the length of the cyclic prefix, and to increase the system's spectral efficiency.

A The log-likelihood function (6)

The log-likelihood function can be written as [6]

$$\Lambda(\theta) = \sum_{k=\theta}^{\theta+L-1} \log\left(\frac{f(r(k), r(k+N))}{f(r(k))\, f(r(k+N))}\right) + \sum_{k} \log f(r(k)) \qquad (10)$$

$$f\left(r(k), r(k+N)\right) = \frac{\exp\left(-\frac{|r(k)-m(k-\theta)|^2 - 2\rho \mathrm{Re}\{(r(k)-m(k-\theta))(r(k+N)-m(k+N-\theta)^*)\} + |r(k+N)-m(k+N-\theta)|^2}{(\sigma_s^2+\sigma_n^2)(1-\rho^2)}\right)}{\pi^2 \left(\sigma_s^2+\sigma_n^2\right)^2 (1-\rho^2)}, \tag{11}$$

where $f(\cdot)$ denotes the probability density function of the variables in its argument.

The two-dimensional density $f(r(k), r(k+N))$ is given in equation (11), where the constant ρ is as defined in (5). The one-dimensional density $f(r(k))$ in (10) is given by

$$f(r(k)) = \frac{1}{\pi\left(\sigma_s^2+\sigma_n^2\right)} \exp\left(-\frac{|r(k)-m(k-\theta)|^2}{(\sigma_s^2+\sigma_n^2)}\right). \tag{12}$$

In three steps, the first term in (10) is now calculated. First, substitution of (11) and (12) yields a sum of a squared form. In the second step we expand and simplify this form by noting that

$$m(k-\theta) = m(k+N-\theta), \quad k \in [\theta, \theta+L-1], \tag{13}$$

due to the cyclic prefix. In the third step we ignore the terms $\sum_{k=\theta}^{\theta+L-1} |m(k-\theta)|^2$ and $\sum_{k=\theta}^{\theta+L-1} \log\left(1-\rho^2\right)$ because they are constants and are not relevant to the maximizing argument of the log-likelihood function. The first term is now proportional to

$$\begin{aligned}\sum_{k=\theta}^{\theta+L-1} \log\left(\frac{f(r(k), r(k+N))}{f(r(k))\, f(r(k+N))}\right) \propto \qquad\qquad (14)\\ \mathrm{Re}\left\{\sum_{k=\theta}^{\theta+L-1} r(k) r^*(k+N)\right\}\\ -\frac{\rho}{2}\sum_{k=\theta}^{\theta+L-1}\left(|r(k)|^2 + |r(k+N)|^2\right)\\ -(1-\rho)\,\mathrm{Re}\left\{\sum_{k=\theta}^{\theta+L-1}\left[r^*(k) + r^*(k+N)\right] m(k-\theta)\right\}.\end{aligned}$$

Similarly, the second term in (10) can be calculated, noting again that some terms in the expansion are independent of θ and do not affect the maximizing argument of the log-likelihood function. From these calculations, the log-likelihood function consists of the three terms in (15) and the additional term

$$\frac{1-\rho^2}{\rho} \mathrm{Re}\left\{\sum_k r(k) m^*(k-\theta)\right\}. \tag{15}$$

Expression (8) now follows readily.

References

[1] 'Digital Video Broadcasting (DVB); Framing structure, channel coding and modulation for digital terrestrial television', European Telecommunications Standard EN 300 744 v 1.1.2, 1997.

[2] Concept group Beta, 'OFDMA Evaluation Report – The multiple access proposal for the UMTS Terrestrial Radio Air Interface (UTRA)', Tdoc/SMG 896/97, ETSI SMG meeting no. 24, Madrid, December 1997.

[3] Broadband Radio Access Networks (BRAN); 'Inventory of broadband radio technologies and techniques', ETSI Technical Report, DTR/BRAN-030001, 1998.

[4] O. Edfors, *Low-complexity algorithms in digital receivers.*, PhD thesis 1996:206, Luleå University of Technology, Sep 1996.

[5] P. Hoeher, 'TCM on frequency-selective land-mobile fading channels', In *Proc. of the 5th Tirrenia International Workshop on Digital Communications*, pp. 317–328, Tirrenia, Italy, September 1991.

[6] J. J. van de Beek, M. Sandell, and P. O. Börjesson, 'ML Estimation of timing and frequency offset in OFDM systems', *IEEE Trans. Signal Proc.*, Vol. 45, no. 7, pp. 1800–1805, July 1997.

[7] L. Wei and C. Schlegel, 'Synchronization requirements for multiuser OFDM on satellite mobile and two-path Rayleigh fading channels', *IEEE Trans. Communications*,Vol. 43, no. 2/3/4, pp. 887–895, Feb/Mar/Apr 1995.

[8] T. Pollet and M. Moeneclaey, 'Synchronizability of OFDM signals', In *Proceedings of GLOBECOM'95*, Vol. 3, pp. 2054–2058. IEEE, November 1995.

[9] J.A.C. Bingham, 'Multicarrier modulation for data transmission: An idea whose time has come', *IEEE Communications Magazine*, Vol. 28, no. 5, pp. 5–14, May 1990.

[10] P. Billingsley *Probability and Measure, Second edition*, John Wiley and Sons, New York, 1986.

[11] W. C. Jakes, *Microwave Mobile Communications*, Classic Reissue, IEEE Press, Piscataway, New Jersey, 1974.

[12] J.J. van de Beek, P.O. Börjesson, M.L. Boucheret, J. Martinez Arenas, D. Landström, P. Ödling, C. Östberg, M. Wahlqvist, and S.K. Wilson, 'A Time and Frequency Synchronization Scheme for Multiuser OFDM', Research Report 1998:06, Division of Signal Processing, Luleå University of Technology, 1998.